ORIGINAL ARTICLE

Lucia Banci · Ivano Bertini · Isabella C. Felli
Ludwig Krippahl · Karel Kubicek · José J. G. Moura
Antonio Rosato

A further investigation of the cytochrome b_5–cytochrome c complex

Abstract The interaction of reduced rabbit cytochrome b_5 with reduced yeast iso-1 cytochrome c has been studied through the analysis of ^1H–^{15}N HSQC spectra, of ^{15}N longitudinal (R_1) and transverse (R_2) relaxation rates, and of the solvent exchange rates of protein backbone amides. For the first time, the adduct has been investigated also from the cytochrome c side. The analysis of the NMR data was integrated with docking calculations. The result is that cytochrome b_5 has two negative patches capable of interacting with a single positive surface area of cytochrome c. At low protein concentrations and in equimolar mixture, two different 1:1 adducts are formed. At high concentration and/or with excess cytochrome c, a 2:1 adduct is formed. All the species are in fast exchange on the scale of differences in chemical shift. By comparison with literature data, it appears that the structure of one 1:1 adduct changes with the origin or primary sequence of cytochrome b_5.

L. Banci · I. Bertini (✉) · I. C. Felli · K. Kubicek · A. Rosato
Magnetic Resonance Center (CERM), University of Florence,
Via Luigi Sacconi 6, 50019 Sesto Fiorentino, Italy
E-mail: bertini@cerm.unifi.it
Tel.: +39-055-4574272
Fax: +39-055-4574271

L. Banci · I. Bertini · A. Rosato
Department of Chemistry, University of Florence,
Via della Lastruccia 3, 50019 Sesto Fiorentino, Italy

L. Krippahl · J. J. G. Moura
Departamento de Química,
Centro Química Fina e Biotecnologia,
Faculdade de Ciências e Tecnologia,
Universidade Nova de Lisboa,
2825-114 Caparica, Portugal

Abbreviations HSQC: heteronuclear single quantum correlation spectroscopy · MD: molecular dynamics

Introduction

Proteins often interact with other proteins to perform their biological function. Quite often such interactions are weak for reasons of reversibility, which is a physiological requirement. Instantaneous complexes are difficult to study, as they rarely crystallize. In addition, in these cases, the complexes in crystals may not be in a biochemically relevant conformation, also because of packing forces. An alternative is that of monitoring a biological function as it depends on specific amino acids, which are substituted by site-directed mutagenesis. Another possible approach is based on bioinformatic tools that permit the prediction of the interaction sites. Finally, NMR spectroscopy can detect the regions of interaction by monitoring chemical shifts. Of course, a combination of the above methods provides the most reliable results.

In the history of the investigation of protein–protein interactions, the case of cytochrome b_5 and cytochrome c has been intensively studied [1, 2, 3, 4, 5]. Cytochrome b_5 is a negatively charged protein at physiological pH, whereas mitochondrial cytochrome c is largely positive. The latter is capable of oxidizing the former in vitro, thus indicating that indeed some kind of interaction has to occur. A structural model of the adduct between cytochrome c and cytochrome b_5 was produced in 1976 [1] that stimulated a lot of further studies. Many experimental techniques (kinetic studies, electrochemistry, site-directed mutagenesis, fluorescence quenching, potentiometric titrations, cross linking) and theoretical approaches (molecular dynamics, Brownian dynamics) were then employed to characterize recognition and electron transfer processes between these two proteins [2, 3, 4, 5, 6, 7]. All these studies clearly point out that the interaction is mainly driven by electrostatic terms

but open questions on the details of the interaction still remain. It has been suggested by several researchers that alternative complex geometries to the one designed by Salemme [1] should be invoked to explain experimental results, as well as the fact that more than one complex configuration could be present in solution [7, 8]. Flexibility of electron transfer protein–protein complexes, as opposed to a tight specific binding, as well as local mobility have also been proposed [8, 9, 10]. In this field, ^{1}H NMR spectroscopy provided evidence of the interaction through chemical shift analysis, first through hyperfine-shifted signals [11, 12] and then through 2D ^{1}H NMR spectroscopy. In particular, ^{1}H NMR pointed out key residues experiencing chemical shift changes upon complex formation and provided information about the binding affinity. Indeed, in the possibility of multiple binding sites, the formation of a ternary complex has been suggested [11], later supported by observations at high concentrations of cytochrome c [13]. This hypothesis was strongly criticized [4] and a 1:1 complex was then nearly always assumed. Later, as ^{15}N-enriched cytochrome b_5 became available, heteronuclear single quantum correlation spectroscopy (HSQC) experiments were performed in the presence of cytochrome c [14, 15] in an attempt to characterize the interaction surface of cytochrome b_5. As a result of this large amount of data from different sources, a number of similar models for the interaction have been proposed in the literature as well as the possibility of multiple binding sites.

A ^{1}H–^{15}N NMR investigation of cytochrome c interacting with cytochrome b_5 is lacking because, until recently, it was difficult to express cytochrome c in conditions and with yields suitable to label it with [15]N. The recent availability of protocols for cytochrome c expression in *Escherichia coli* [16], enabling the correct covalent attachment of the heme cofactor to the protein frame, prompted us to re-examine the cytochrome b_5–cytochrome c complex. The system was studied with both proteins in the reduced state since it was impossible for us to keep one or both proteins in the oxidized state for the long time of the NMR experiments. The characterization of these adducts still has a biological meaning, as the surfaces and their electrostatic potentials are not affected by the redox state (as witnessed by the comparison of the structures in the two states [17, 18, 19, 20]) and therefore are expected to provide relevant information about the adducts. [15]N chemical shifts were monitored through ^{1}H–^{15}N HSQC experiments, which are very sensitive and thus relatively quick. The characterization of the interaction between the proteins and the solvent provided information complementary to that of chemical shift mapping. Finally, the ratio between transverse and longitudinal relaxation rates (R_2/R_1) provided information on the stoichiometry and overall shape of the complex. A recently developed computer program [21] allowed us to use the NMR data to provide a model of the interaction. In a similar approach, heteronuclear NMR and docking calculations were used for building structural models of the cytochrome c_{553}–ferredoxin complex and a combination of TROSY experiments and docking calculations were used for the study of the [Fe]-hydrogenase–cytochrome c_{553} complex [22, 23]. Other, more recent, applications of similar strategies include the cytochrome b_5–myoglobin [24] and the cytochrome c–cytochrome f [25] complexes. The present approach can thus be seen as a general strategy for the investigation of adducts between electron transfer proteins.

Materials and methods

Sample preparation

Cytochrome b_5 was isolated and purified from the TOPP2 *E. coli* strain hosting the plasmid pKK223-3 that encodes the soluble domain (98 amino acids) of rabbit cytochrome b_5 (kindly provided by A.W. Steggles, Northeastern Ohio Universities College of Medicine, Ohio, USA) following a procedure already reported [26]. Both ^{15}N and doubly labelled ^{15}N/^{13}C samples were prepared as previously described [27].

Cytochrome c was expressed and purified from BL21(DE3)C41 *E. coli* competent cells hosting the plasmid pEC86 [28], which expresses the *ccm* genes under the control of the *tet* promoter, and the pMSV1 plasmid encoding the ADL C102T yeast iso-1-cytochrome c [16]. The detailed procedure to obtain unlabeled and ^{15}N-labelled protein samples has been already described [16].

10% D_2O was added to each NMR sample for the lock signal. The samples were handled in a glove box under a N_2 (90%)/H_2 (10%) atmosphere to maintain anaerobic conditions and the NMR tubes were sealed with Teflon caps before removing from the glove box. Reduction of both cytochromes was achieved by addition of a 0.2 M sodium dithionite solution in order to have a slight excess of reductant compared to the concentration of protein. The final pH was checked throughout each titration step and kept within the range 7.1–7.2. The protein concentrations of ^{15}N-labelled NMR samples were estimated by UV/Vis spectroscopy using available extinction coefficients for reduced cytochrome b_5 [26] and cytochrome c [29], respectively. NMR titrations were performed in a strictly anaerobic environment (see above) by addition of the ^{15}N-enriched partner to the other, unlabelled sample. Typically, the molar ratio between the two proteins was varied during the titration from 0 to 1.5, in five or six iterations. Each point in the various titrations was repeated twice to check the reproducibility of complex formation. No buffer was used, and the pH values of the samples were adjusted by additions of small quantities of concentrated NaOH or HCl solutions, as needed.

NMR experiments

NMR experiments were acquired at 298 K using Bruker instruments of the Avance series operating at 16.4 T (700 MHz) and 18.8 T (800 MHz). All NMR spectrometers were equipped with ^{1}H,[13]C,[15]N TXI probes with z-pulsed field gradients. Cytochrome b_5 is present in solution in two isomers that differ by a 180° rotation of the heme plane [30]. The ratio of the two isomers in the rabbit protein is about 9:1 [20]. Only the resonances belonging to the major isomer were analysed.

The 3D CBCA(CO)NH [31] and CBCANH [32] NMR experiments, acquired at 800 MHz, were used to assign the NH resonances (^{1}H and ^{15}N) of the reduced form of rabbit cytochrome b_5. Sensitivity improved, echo-anti-echo HSQC experiments [33, 34] were acquired to follow ^{1}H and ^{15}N chemical shift changes throughout the titrations. [15]N R_1 and R_2 relaxation rates were measured using available pulse sequences at 11.7 T (50 MHz for [15]N Larmor frequency), through, respectively, inversion-recovery [35] and CPMG measurements [36]. In all experiments, solvent suppression was achieved with the water flip-back scheme, which avoids water saturation [37]. R_1 and R_2 relaxation rates were

obtained by fitting the cross-peak volumes (I), measured as a function of the relaxation delay, to a single exponential decay. Intensities at 10 different delays were acquired for both R_1 and R_2 measurements. The diffusion anisotropy of the molecules in solution was calculated from the local τ_m values derived from the R_2/R_1 ratio of each individual residue [38], using the program quadric_diffusion [39]. Inertia moments were calculated with the program pdb_inertia [39]. CLEANEX experiments [40] were performed in order to monitor the accessibility of amide moieties to the solvent in the two separate proteins and in equimolar mixtures of them.

For 2D experiments, the experimental data were processed with 2048×512 data points in the ^{1}H and ^{15}N dimensions, respectively, using the programs Xwinnmr and NMR-pipe [41]. Resonance assignment was performed using the program Xeasy [42] and part of the analysis was done with the program Sparky [43].

Data analysis and calculations

For analyses, it is useful to define a "combined chemical shift variation". This is calculated from the experimental ^{1}H and ^{15}N chemical shift variations [$\Delta\delta(^1$H) and $\Delta\delta(^{15}$N), respectively] measured between corresponding peaks of the isolated protein and the protein in an equimolar mixture with its partner, through the following equation [44, 45]:

$$\Delta\delta^{\text{combined}} = \sqrt{\frac{(\Delta\delta(^1\text{H}))^2 + \frac{1}{25}(\Delta\delta(^{15}\text{N}))^2}{2}} \tag{1}$$

Protein docking calculations

Docking calculations were carried out with the program BiGGER 2.0 [21], which requires as input a 3D structure for each of the two interacting proteins. The structure of the complex is then calculated through a soft-docking approach. Here, calculations were performed using the energy-minimized average solution structures for both free cytochrome c [17] and cytochrome b_5 [20]. The calculation procedure is divided in two steps called "searching" and "scoring". In the first step the program generates a population of docked geometries with maximal surface matching. Each protein is converted into a matrix of cubic cells of 1 Å^3 size (digitization) and then one of the two matrices (probe) is translated with respect to the other (target) to obtain optimal surface matching. The probe is then rotated by 12° with respect to the target and the digitization–translation–surface matching process is repeated, until a complete search of the interaction space is achieved. The program simulates a certain degree of flexibility for surface side chains Arg, Lys, Asp, Glu and Met, by allowing them to penetrate up to the core of the other protein. The result of this procedure is an ensemble of 5000 possible model structures for the complex, selected on the basis of best surface matching.

For subsequent analyses, the 5000 model structures in the above ensemble are ranked based on computational and/or experiment-based score functions [21]. To this end, a so-called global scoring function, defined from the combination of several terms, is computed by the program [21]. Note that this global score is generated by BiGGER using some energetic contributions (such as electrostatic interactions and solvent exclusion effects) but also many other factors that cannot be converted directly in energy terms, such as surface complementarity or statistics on side chain contacts. All these factors are aggregated by a neural network classifier that was trained and tested on known complexes, to provide a general ranking of the models generated in the absence of additional information [21]. As a consequence, the results of BiGGER cannot be used to derive quantitative energy estimates for the energetics of interaction. An alternative scoring function ("NMR filter") has been defined by using the results of chemical shift mapping. To compute the NMR filter, combined chemical shift variations larger than the average were considered as arising from protein–protein interactions. Amide moieties experiencing variations above this threshold in either cytochrome c or cytochrome b_5 were thus selected for application of the NMR filter in BiGGER calculations, resulting in an ensemble of "interacting atoms" for each protein. The filter was built by considering all possible pairs constituted by one atom from each of the two ensembles, and then evaluating the average of all interatomic distances for these pairs. The value of this score is thus lower the closer are the "interacting atoms" in one protein to the "interacting atoms" in the other protein. The NMR filter was applied to all the 5000 structures produced by BiGGER. Other possible definitions of the NMR filter, e.g. by assuming that all atoms experiencing a significant chemical shift variation should be closer than a given cut-off to an atom of the other protein, and then ranking the complexes by the number of violations of these NMR constraints, produced results similar to those of the presently defined filter.

The solutions of BiGGER most representative of the structure of the adduct (see Results) were subjected to energy minimization through the Sander module of the AMBER 6.0 software package [46] with standard procedures [47], using the force field parameters for the heme previously derived for cytochromes [19, 48].

Results

NMR experiments

Assignment of the resonance of the backbone atoms in reduced rabbit cytochrome b_5 was achieved through the 3D NMR CBCA(CO)NH and CBCANH experiments, and is reported in the Supplementary material. In total, 95% of the residues in the segment 1–89 were assigned (H^N, N, C$^\alpha$ and C$^\beta$). The assignment of amide groups of reduced cytochrome c was taken from the literature [16].

Upon addition of the unlabelled protein partner, only shift changes are detected for the ^{15}N-enriched proteins and no additional peaks are observed through the NMR titrations. This behavior indicates that there is an interaction between the two proteins, and that the kinetics of the association and dissociation of the two partners is fast on the chemical shift time scale. Chemical shift changes for the backbone ^{1}H^N and ^{15}N nuclei were followed throughout titrations in which one of the two proteins (unlabelled) was added to the other (^{15}N-labelled). The combined chemical shift changes observed for reduced cytochrome b_5 and for reduced cytochrome c upon complex formation are shown in Fig. 1. The mean combined chemical shift variations were 0.026 ± 0.024 ppm for cytochrome b_5 and 0.033 ± 0.028 ppm for cytochrome c. For a number of residues in both proteins the profile of chemical shift variations as a function of the molar ratio of the two proteins did not match well what was expected on the basis of the formation of a 1:1 adduct (or of different 1:1 adducts in equilibrium), suggesting that a 1:2 adduct may also be formed in solution [13] (see later). Fittings of the titrations (not shown) indicate that the association constant for binding of the second cytochrome c molecule is slightly more than one order of magnitude smaller than that for binding of the first molecule.
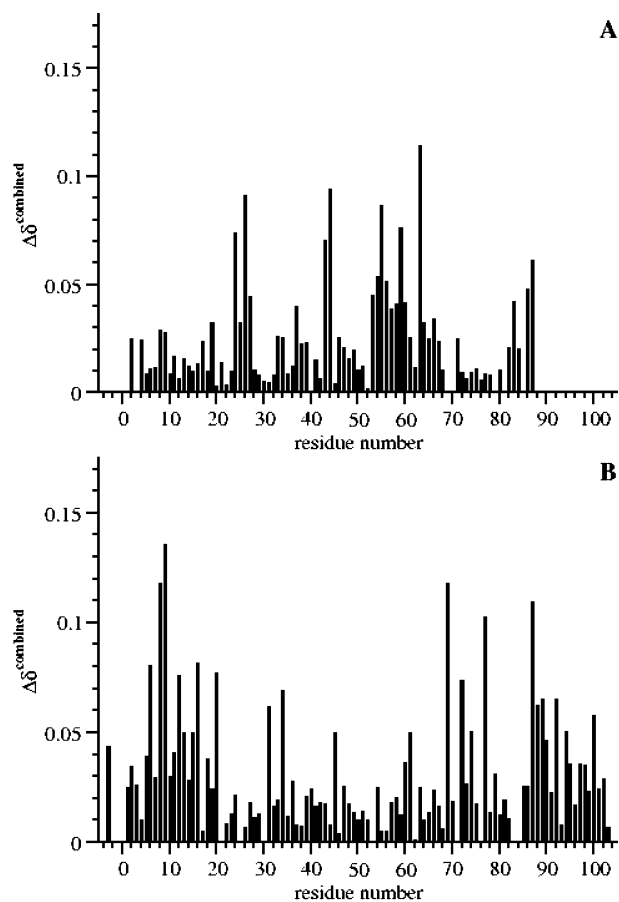
Fig. 1 Combined chemical shift changes, as defined by Eq. 1, of ^{15}N and ^{1}H backbone amide nuclei in reduced cytochrome b_5 (**A**) and reduced cytochrome c (**B**) upon binding to the reduced partner

Fig. 2 Combined chemical shift changes in each protein upon complex formation are mapped (*central panels*) on the protein 3D solution structures (*upper panels*) [17, 20]. The backbone, the heme and the two axial ligands are shown. The color of the spheres is proportional to the magnitude of chemical shift change (*from red to white*, with *red* corresponding to the largest absolute variation). In the *bottom panels*, the results of CLEANEX experiments are shown: residues in *cyan* are those exchanging with the solvent both in absence and in presence of the partner; residues in *blue* (labelled) exchange in absence of the partner, but are protected from exchange in presence of the partner

Combined chemical shift changes are mapped onto the protein solution structures in Fig. 2. The largest changes are clustered in specific regions of the proteins. For cytochrome b_5, they are found for residues 8–9, 19, 24–27, 37, 43–44, 53–60, 63–66, 83 and 86–87. The majority of these form the heme-binding pocket. In particular, residues 24–27 belong to the part of the β-sheet of cytochrome b_5 which is at the back of the heme cavity. The other residues are located in the four helices (α_2 to α_5 [20]) making up the heme-binding pocket, with residues in helix α_4 (spanning residues 52–62) displaying the largest chemical shift changes. The N-terminal part of helices α_3 and α_5 (which comprise residues 42–49 and 64–74, respectively) are also somewhat affected by the interaction. On the other hand, smaller chemical shift variations are observed for the amide moieties in helix α_2 (which involves residues 33–39). In cytochrome c, the largest combined shift variations are located in two α helices, α_1 (4–13) containing two positively charged lysines, and α_4 (90–101), i.e. in the N- and C-terminal helices. These helices are in contact, the angle between their axes being close to 90°. The residues involved in inter-helical interactions are, respectively, 6, 7 and 10, and 93, 94, 97 and 98 [17]. These contacts are very well conserved in the mitochondrial
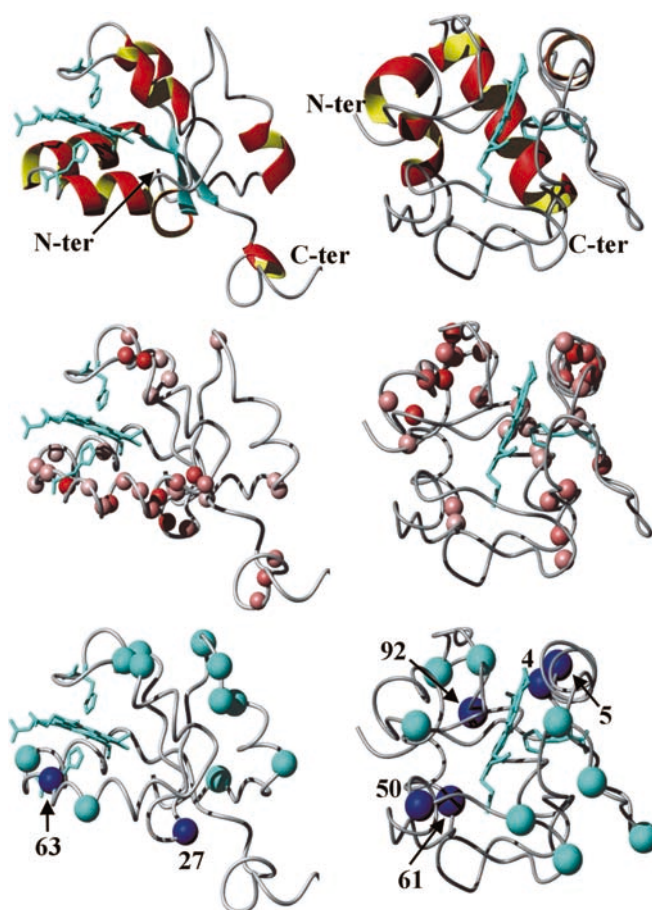
cytochrome c family [49, 50]. Other residues with sizable chemical shift changes are 15–20, 31, 34, 45, 60–61, 69, 72, 74, 77 and 87–89 (Fig. 1). Residues 15–20 and 87–89 are spacially close to the above-mentioned helices as well as residues 31, 34, 45, 60, 61 and 74.

CLEANEX experiments [40] were performed to monitor the change in hydration properties of the two proteins upon complex formation. Indeed, it is expected that amide moieties in regions involved in specific intermolecular contacts would become protected from exchange with H_2O upon interaction with the partner. Unfortunately, no information can be obtained for those amide groups which exchange slowly (i.e. on a time scale longer than minute) with the solvent in the isolated protein, i.e. several of those in regions with regular secondary structure, which cannot be observed in CLEANEX spectra. In the case of cytochrome c, these experiments show that the amide moieties of residues 4,

5 and 92, and, to a smaller extent, 50 and 61, become protected from the solvent upon interaction with cytochrome b_5 (Fig. 2). For cytochrome b_5, protection upon interaction with the partner is observed for residues 27 and 63 (Fig. 2). It is worth noting that variations in the behavior of amide moieties in CLEANEX experiments could be due to either direct steric protection from the solvent caused by the formation of the adduct or to conformational rearrangements which result in enhanced protection.

^{15}N R_2/R_1 ratios can provide information about the size and shape of macromolecular adducts in solution, as they are a function of the correlation time, τ_m, for molecular tumbling and of the anisotropy of diffusion. Therefore ^{15}N R_2/R_1 ratios were measured on the isolated proteins as well as on a number of protein mixtures with different protein concentrations and/or different molar ratios, with the aim to characterize the molecular weight of the adduct, and its dependence on solution composition. R_2 and R_1 values of the n-th residue were used for analysis if the following criterion was satisfied [51]: $(<T_2> - T_{2,n})/<T_2> - (<T_1> - T_{1,n})/<T_1> > 1.5 \times$SD, where $T_{2,n}$ and $T_{1,n}$ are the T_2 ($=1/R_2$) and T_1 ($=1/R_1$) values of residue n, and $<T_2>$ and $<T_1>$ are the average values over all residues. This criterion excludes from the analysis the residues whose R_2 has a significant contribution due to chemical exchange [51]. About 65% of the residues satisfied this criterion for both cytochrome b_5 and cytochrome c in the various conditions investigated. The correlation time for molecular tumbling in solution was estimated to be 5.5 ns and 6.2 ns for isolated cytochrome b_5 and cytochrome c, respectively. The correlation times observed in the various mixtures are shown in Table 1. It can be seen that for equimolar mixtures the measured correlation time for molecular tumbling is essentially identical to the sum of the correlation times of the isolated proteins. However, in the presence of an excess of cytochrome c, the correlation time increases significantly with respect to what observed in equimolar mixtures. This increase is higher the higher the concentration of the proteins, and the higher the ratio between the concentrations of cytochrome c and cytochrome b_5. Overall, the data of Table 1 indicate that in the protein concentration range

0.2–1.3 mM, in solution there are multiple equilibria, involving formation of 1:1 as well as 1:2 cytochrome b_5–cytochrome c adducts. Interestingly, in a quite recent study, two binding site for cytochrome c were identified on cytochrome f, involved in formation of a non-physiological complex [25].

For cytochrome c the axial anisotropy of the diffusion tensor ($D_{||}/D_\perp$) measured in an equimolar mixture with cytochrome b_5 is roughly 1.3. The orientation of the principal axis of the tensor of cytochrome c suggests that the region of interaction comprises residues 5–15 and 85–90. There is good agreement between the direction of the diffusion tensor axis and the axis of the inertia tensor of the most representative complexes calculated by BiGGER, and identified by the intersection of the electrostatic score and the NMR filter (see next section). Also the anisotropy of the diffusion tensor is in keeping with expectations based on the inertia tensor. The axial anisotropy observed for cytochrome b_5 is instead smaller than 1, which is not consistent with the presence in solution of a single 1:1 adduct, but can arise from the presence of simultaneous equilibria involving different 1:1 and/or 1:2 adducts.

Docking calculations

The 5000 structural models generated for the cytochrome b_5–cytochrome c complex were ranked using the global scoring function. Inspection of the 100 highest-ranking complexes did not provide a single, even low-resolution, complex. Rather, both cytochrome b_5 and cytochrome c showed a few different possible alternatives for the interaction surface (represented by highly populated clusters of putative solutions). This is often observed in BiGGER calculations [21]. The opposite, sizeable charge on the two partners suggests that recognition between the two proteins is likely to occur through electrostatic interactions. This is in agreement with the dependence of the dissociation constant on the ionic strength of the solution [52]. Thus, it is a plausible option to rank the complexes on the basis of electrostatic interaction alone, rather than on the basis of the global scoring function. If this is done, the 100 highest-ranking solutions out of the 5000 calculated feature a somewhat different population of the various putative interaction sites, with respect to ranking by the global scoring function. However, a unique cluster of solutions for the complex is still not obtained. A third alternative approach is that of using the NMR filter to directly rank the 5000 BiGGER solutions, and then analyze the best 100 solutions. Also this procedure does not provide a unique model for the complex structure, but rather highlights different possible interaction patches on cytochrome b_5 and on cytochrome c (Fig. 3). A combined scoring of the solutions calculated by BiGGER can be obtained by performing, for example, an intersection of the 100 solutions with best electrostatic score and of the 100 solutions with best values for the NMR

Table 1 Isotropic correlation times (τ_m) for molecular tumbling measured from ^{15}N relaxation rates in different mixtures of cytochrome b_5 and cytochrome c. In all cases, only one the two proteins was enriched in ^{15}N (indicated in the "Observed" column) and thus used for calculations

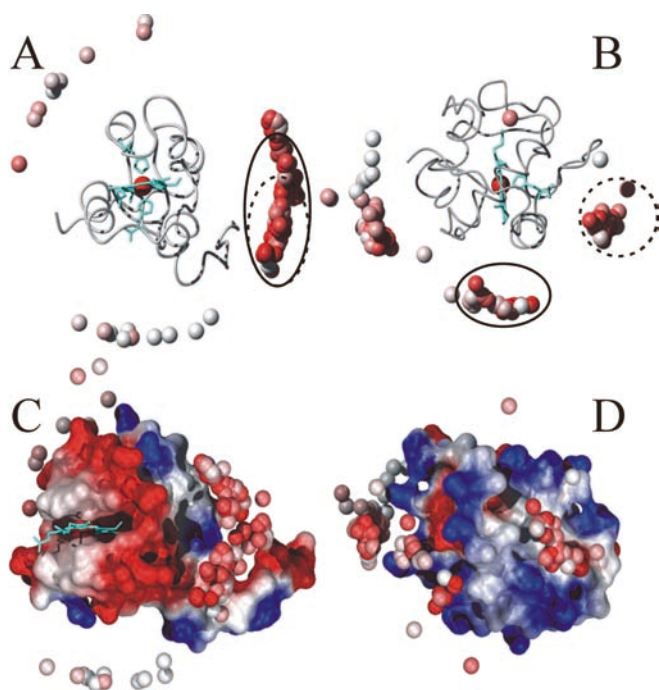| Total concentration of cytochrome c (mM)	Total concentration of cytochrome b_5] (mM)	Observed	Molar ratio (c:b_5)	τ_m (ns)
0.63	0.64	b_5	1.0	11.7 ± 1.2
1.28	0.81	b_5	1.6	16.3 ± 1.8
0.35	0.23	b_5	1.5	13.3 ± 0.8
0.28	0.27	c	1.0	11.7 ± 1.1
0.23	0.31	c	0.7	12.1 ± 1.1

Fig. 3 Display of the complexes calculated by BiGGER showing (**A**) the backbone trace of cytochrome b_5 superimposed with the position of the center of mass of cytochrome c in the 100 putative solutions with best value of the NMR filter. The solutions are colored according to their value (*from red to white*: best agreement to worst agreement). (**B**) The same as **A**, but with cytochrome c at the center. *Dotted circles*: intersection of the ensemble of the 100 solutions with best NMR filter with the ensemble of the 100 solutions with best BiGGER global score. *Solid line circle*: intersection of the ensemble of the 100 solutions with best NMR filter with the ensemble of the 100 solutions with best BiGGER electrostatic score. (**C**) The electrostatic potential surface of cytochrome b_5 (rotated with respect to **A** in order to allow the reader to look at the interaction regions; *blue*: positive charge, *red*: negative charge). (**D**) The electrostatic potential surface of cytochrome c (rotated with respect to **B** in order to allow the reader to look at the interaction regions)

filter (Fig. 3). This latter approach provides a smaller ensemble of possible solutions, which can then be manually inspected and selected based on their agreement with the remainder of the NMR data available from CLEANEX experiments and ^{15}N relaxation rate measurements (see Discussion).

Discussion

Characterization of the adduct(s) between cytochrome c and cytochrome b_5

In the present work, the interaction between cytochrome c and cytochrome b_5, which constitutes a paradigm for protein–protein interactions involving electron transfer proteins, has been investigated through heteronuclear NMR, using both partners in the reduced Fe^{2+} state. While stable isotope enrichment of cytochrome b_5 has been possible for several years, it is only recently that expression systems enabling stable isotope enrichment of

cytochrome c have become available [16, 28, 53, 54]. Consequently, we have taken advantage of this new possibility to obtain further insights on the present system, by monitoring the interaction from the point of view of both partners. Indeed, previous structural studies by NMR (the only technique capable to provide structural information at atomic level on protein adducts in which there is fast equilibration between the free and bound proteins) had mainly focused on the analysis of cytochrome b_5, with only a few exceptions [4].

Our results indicate that, under the present experimental conditions, cytochrome b_5 and cytochrome c can form both a (or multiple) 1:1 adduct and a 1:2 adduct. This is consistent both with chemical shift variation profiles observed in titrations and with the observed molecular tumbling rates of Table 1. Having both proteins almost equal in mass, the formation of a 1:1 adduct would cause doubling of the molecular mass of the species observed, which implies a doubling of the tumbling correlation time. Anisotropic tumbling of the complex in solution can yield up to an additional 15% increase in this correlation time [55]. In our case, the observed values of τ_m are sizably larger, indicating the presence of an equilibrium involving adducts of mass larger than the double of each protein. A similar contention was proposed earlier [11, 13], based on NMR data, and later criticized [4]. ^{15}N relaxation data provide a direct indication of the size of the adduct(s) in solution and are thus reliable indicators of the stoichiometry of the complex. It is worth noting that part of the criticisms invoked the possibility of paramagnetic relaxation mechanisms to justify linewidths larger than expected [4]. In our study, performed on the reduced proteins, relaxation rates are only determined by diamagnetic relaxation mechanisms and therefore larger rates can only originate from a longer tumbling correlation time. This confirms the 1:2 complex formation. Unsurprisingly, the population of the 1:2 adduct decreases rapidly with decreasing concentration, making its detection impossible when working at micromolar concentrations, as is the case of measurements performed by electronic spectroscopy, or even with dilute NMR samples. The dissociation constant for the second cytochrome c molecule is indeed estimated to be in the millimolar range, which also suggests that the 1:2 adduct might not have any physiological relevance.

The surface regions involved in the interaction for the two partners can be identified by mapping chemical shift variations on the two interacting proteins [56]. CLEANEX experiments can provide complementary information by monitoring changes in protein–solvent interaction upon complex formation. Both chemical shift mapping and CLEANEX suffer from a common shortcoming, that is they cannot distinguish between direct effects due to intermolecular interactions and intramolecular conformational rearrangements. In the case of the adduct formed by reduced cytochrome c and cytochrome b_5, a single interaction patch is identified on

cytochrome c, while the picture is more complex for cytochrome b_5 (Fig. 2). Indeed, as described in the Results section, the regions experiencing large chemical shift variations on the surface of cytochrome b_5 are far in space from one another, so that it is not possible to rationalize the observed changes by assuming that they result from a single interaction with a molecule of cytochrome c. Given the fact that NMR relaxation data indicate that an adduct (cytochrome b_5)–(cytochrome c)$_2$ can be formed in solution, it can be proposed that there are two different interaction regions on cytochrome b_5, which can be affected simultaneously (the right and bottom parts displayed in Fig. 3A). The existence of different interaction regions on cytochrome b_5 has already been proposed [15, 57]. The above findings are also in agreement with the diffusional properties of the molecules in the adduct, obtained from ^{15}N relaxation data using well-documented approaches [38, 39, 58]. The diffusion tensor obtained for cytochrome c in the complex is in agreement with binding by cytochrome b_5 occurring at only one site, while the tensor for cytochrome b_5 suggests that binding by the partner occurs at more than one site.

Soft docking calculations performed with the program BiGGER [21] resulted in a variety of different possibilities for the structure of the adduct between cytochrome c and cytochrome b_5. As mentioned in the Methods section, each of these structures is assigned by BiGGER a so-called global score, which indicates how well it complies with parameters such as surface complementarity, or statistics on side-chain contacts derived from available structures of protein–protein complexes [21]. Consequently, the global score cannot be correlated with binding energy. The selection of models therefore must be carried out by integrating calculations with experimental data, which is done by ranking the results based on the chemical shift variation data (Fig. 3). From Fig. 3 it appears that the application of the NMR filter does leave some ambiguity on the configuration of the adduct. The NMR filter is based on the assumption that the amide moieties experiencing large combined chemical shift variations (i.e. larger than average combined chemical shift difference) should be close to the protein–protein interaction region. The fact that from BiGGER calculations it is not possible to obtain structures in which all protein residues experiencing large shifts are close to a single interface is thus consistent with the considerations already outlined in this section. Notably, the interaction patch identified by chemical shift mapping on the cytochrome c surface corresponds to different clusters of solutions (which are close in space) in BiGGER calculations (Fig. 3). The intersection of the 100 solutions with best BiGGER global score with the 100 solutions with best agreement with the NMR filter (defined in Methods) results in an ensemble of nine similar solutions, corresponding to only one of the mentioned different clusters (dotted circle in Fig. 3B). The putative interaction region in this ensemble has an electrostatic potential at the surface close to zero (Fig. 3D), i.e. it is hydrophobic. However, this region does not comprise the residues of cytochrome c showing enhanced protection from the solvent in the adduct. On the other hand, if the electrostatic score computed by BiGGER is intersected with the NMR score, a second cluster of solution is selected (solid circles in Fig. 3), where the residues with enhanced protection in the adduct (based on CLEANEX experiments) are at the intermolecular interface. Notably, the latter cluster of solutions comprises those with the best agreement with the chemical shift data among all the 5000 solutions computed by BiGGER, and corresponds to a region with significant electrostatic potential at the surface (Fig. 3D). As mentioned, the directions of the axes of the inertia tensor for the structures of the complex in the group of solutions resulting from the combination of the electrostatic and NMR scores are in good agreement with the directions of the diffusion axis obtained from ^{15}N relaxation data on cytochrome c. This observation suggests that they are representative of the configuration of cytochrome c within the adduct in solution. For cytochrome b_5, the intersection of either the global or electrostatic score computed by BiGGER with the 100 solutions best satisfying the NMR filter defines the same configuration for interaction with cytochrome c (Fig. 3). This is also the configuration corresponding to the best values of the NMR filter. On the other hand, as discussed, the data of Table 1 and the profiles of chemical shift variations indicate that a second protein region should be simultaneously involved in the interaction. Among the solutions calculated by BiGGER, there are at least two other clusters of solutions in agreement with NMR data, besides the one identified by the intersection of the NMR and global scores (solutions below and at the left of cytochrome b_5 in Fig. 3A). Either of these two clusters can correspond to the second interaction region in the (cytochrome b_5)–(cytochrome c)$_2$ adduct. The presently available data do not allow us to definitely discriminate between these two clusters. However, it is worth noting that the most highly charged regions of the electrostatic surface of cytochrome b_5 (Fig. 3B) are those corresponding to the right (already identified as being a region of intermolecular interaction) and bottom faces of the protein in the orientation of Fig. 3A. Since the role of electrostatics appears to be crucial in driving the formation of the complex, it is tempting to propose that the bottom cluster of solutions identifies the second interaction region on cytochrome b_5 (see Fig. 3A and Fig. 3C). As far as electron transfer is concerned, there are no peculiar features in either of the two possible complexes suggesting a significant difference in reactivity.

Comparison with previous studies

The chemical shift changes observed for reduced rabbit cytochrome b_5 in this work show some potentially relevant differences with similar data recently reported for

reduced bovine cytochrome b_5 [15]. In the present study, the region 10–20 (which comprises part of the first α-helix and of the first strand of the β-sheet backing the heme cofactor) displays quite small chemical shift variations upon interaction with cytochrome c, while in the previous study it was one of the regions most affected by the interaction with cytochrome c [15]. The amino acid sequence of the rabbit (used in this work) and bovine (used in the previous study) proteins in this region differ at two positions (out of the six amino acid variations present in the whole sequence), namely 13 (Lys to Gln) and 17 (His to Asp). Instead, chemical shift variations in the heme-binding pocket (whose sequence is conserved in the rabbit and bovine proteins) indicate in both this work and previously [15] that the region highlighted by the circles in Fig. 3A is a site for interaction. Nevertheless, small differences in the chemical shift variation patterns are observed even in this region, which can be due to either different sample conditions, and/or on the different origin of the partner (recombinant yeast iso-1 cytochrome c was used here, while Hom et al. used horse heart cytochrome c [15]). Additionally, the amino acid variations in the region 10–20 mentioned above induce formation of a different adduct in solution, which in turn causes the observed differences in chemical shift mappings. In this context, it is useful to keep in mind that subtle but significant species-dependent structural differences were also observed by comparing the solid-state structures of cytochrome c peroxidase (CcP) with cytochrome c from either yeast or horse heart [59]. In summary, it appears that one interaction region on cytochrome b_5 is largely independent both of the primary sequence of the protein and its redox state, and coincides with that identified in calculations by intersection of the NMR filter with the BiGGER electrostatic score (dotted circle in Fig. 3A), as both studies find the same region. This comprises helix α_4 (43–48), part of helix α_5 (55–58) and part of the strand formed by residues 23–27. The second interaction region appears instead to be more susceptible to variations in primary sequence. In our case, the most likely additional binding site comprises helix α_5 (55–61) and the turn up to residue 64.

The largest combined chemical shift variations observed on cytochrome c define quite clearly a large single patch on the surface of cytochrome c (Fig. 2). This patch comprises also the residues experiencing the largest enhancement in protection from solvent upon interaction with the partner. For cytochrome c there is no available literature relative to the effect of the interaction with cytochrome b_5 on the chemical shifts of its backbone nuclei. A chemical shift mapping study is instead available on the interaction between oxidized and reduced ^{15}N-enriched yeast iso-1 cytochrome c and unlabelled CcP in the so-called resting state [60]. The largest chemical shift variations were observed for residues 12–16 and the region around Phe82. These regions are close to, but different from, those experiencing the largest shifts in this work (Fig. 1), presumably indicating that

the interaction between cytochrome c and either CcP or cytochrome b_5 does not involve the same surface patch. NMR data on a derivative of horse heart cytochrome c where Lys residues had been dimethylated also support this hypothesis [61].

It is interesting to compare the present results to the so-called Salemme model for the interaction between cytochrome c and cytochrome b_5 [1]. According to this model, which assumes formation of a 1:1 complex, the interaction region of cytochrome b_5 is essentially the one identified presently by the intersection of the BiGGER electrostatic score and the NMR filter (dotted circle in Fig. 3A). As mentioned above for the case of NMR studies, essentially all available experimental studies agree that this is one of the regions directly involved in intermolecular interaction, regardless of the source or oxidation state of the proteins used in experiments. Indeed, replacement of the charged residues 43, 44, 48 and 60 located in this region to their neutral analogues [2] and of 44, 48, 54 and 60 (as well as multiple replacements) to Ala [62, 63, 64] by site-directed mutagenesis in all cases results in an increase of the dissociation constant.

The interface region identified here for cytochrome c is different from that proposed by Salemme [1], and is instead close to the alternative, more stable, structure predicted by Brownian dynamics simulations [7]. It is to be noted that the interaction region of cytochrome b_5 in the latter structure and in the Salemme model are very similar. The results of our CLEANEX experiments give further support to the proposition that the Salemme model does not represent well the dominant configuration of cytochrome c in the adduct in solution, as a number of residues which would be shielded from solvent in the complex proposed by Salemme are found to remain unprotected from solvent in the presence of cytochrome b_5. In the dominant configuration suggested by our data, the iron–iron distance is around 20 Å, as compared to a range from 17 to 38 Å observed in all the 5000 solutions obtained from BiGGER calculations. The closest pair of heme substituents in the family of structures is methyl 3 of cytochrome c and methyl 5 of cytochrome b_5, with the acute angle between the heme planes being around 30°. Side-chain chemical modification studies support the role in inter-protein interactions of residues 13, 27, 72 and 79 of cytochrome c [65, 66], all of which, except 13, are far from the interaction interface. It should be kept in mind that in our calculations the structures of the two proteins are kept rigid, maintaining the conformation observed in solution in the absence of the partner. Some rearrangements could take place in solution, e.g. bringing the side chain of Lys72 of cytochrome c close to heme propionate 6 of cytochrome b_5, as predicted by calculations [7] and also suggested by experiments on cytochrome b_5 [67]. On the other hand, residues 27 and 79 of cytochrome c are too far from the interface in our calculated model to account for their role, proposed on the basis of experimental data, in modulating electron transfer between cytochrome b_5 and cytochrome c. A possible explanation for this finding is

that the complex proposed by Salemme, which is competent for electron transfer, forms dynamically in solution, but only exists for a fraction of time small enough not to give rise to appreciable perturbation of NMR chemical shifts and of ^{15}N relaxation rates. In this respect, it is also worth noting that the interface regions on cytochrome c in the Salemme model and in the electrostatically dominant model are adjacent. The importance of inter-protein dynamics in electron transfer complexes appears to be quite different in different systems [14, 24, 25], but likely plays a crucial role in modulating the rate of the process [68].

Conclusions

Taking advantage of the recent availability of expression systems suitable for stable isotope enrichment of cytochrome c, we have performed a thorough NMR investigation of the interaction between cytochrome c and cytochrome b_5, which constitutes a paradigm for the study of adducts formed by electron transfer proteins. The interaction has been characterized through the analysis of the variations of chemical shifts, of solvent exchange and of ^{15}N relaxation rates of either protein upon addition of the partner in solution. The analysis has been complemented by theoretical calculations with the program BiGGER.

Cytochrome c and cytochrome b_5 have been shown to form multiple adducts in solution, with 1:1 or 2:1 stoichiometry. The adducts are in fast (on the NMR time scale) equilibrium with the unbound proteins. The approach presented in this work permits the identification of the regions of intermolecular interaction with good accuracy, even though the presence of simultaneous equilibria complicates the analysis of the data. This approach appears a suitable general methodology for the investigation of electron transfer complexes. In the present system, complex formation between cytochrome c and cytochrome b_5 appears to be electrostatically driven, in keeping with previous propositions. However, there are indications that short-lived alternate configurations do exist in solution.

The formation of transient complexes might be a requirement in electron transfer proteins in order to have optimal electron transfer. Complexes cannot get stuck in a given rigid conformation as this would require high energy for dissociation and would slow down the entire electron transfer process. As fast exchanging, transient complexes are formed, it might be reasonable that more than one protein conformation/orientation is reached in the protein–protein encounter. Furthermore, it should be kept in mind that cytochrome c interacts with two different partners, one accepting and one donating one electron, for which different binding regions might be favorite.

References

1. Salemme FR (1976) J Mol Biol 102:563–568
2. Rodgers KK, Pochapsky TC, Sligar SG (1988) Science 240:1657–1659
3. Burch AM, Rigby SEJ, Funk WD, MacGillivray RTA, Mauk MR, Mauk AG, Moore GR (1990) Science 247:831–833
4. Mauk AG, Mauk MR, Moore GR, Northrup SH (1995) J Bioenerg Biomemb 27:311–330
5. Durham B, Fairris JL, McLean M, Millet F, Scott JR, Sligar SG, Willie A (1995) J Bioenerg Biomemb 27:331–340
6. Eltis LD, Herbert RG, Barker PD, Mauk AG, Northrup SH (1991) Biochemistry 30:3663–3674
7. Northrup SH, Thomasson KA, Miller CM, Barker PD, Eltis LD, Guillemette JG, Inglis SC, Mauk AG (1993) Biochemistry 32:6613–6623
8. Mauk MR, Mauk AG, Weber PC, Matthew JB (1986) Biochemistry 25:7085–7091
9. Wendoloski JJ, Matthew JB, Weber PC, Salemme FR (1987) Science 238:794–797
10. Whitford D, Gao Y, Pielak GJ, Williams RJ, McLendon GL, Sherman F (1991) Eur J Biochem 200:359–367
11. Miura R, Sugiyama T, Akasaka A, Yamano T (1980) Biochemistry Int 1:532–538
12. Eley CGS, Moore GR (1983) J Biochem (Tokyo) 215:11–21
13. Whitford D, Concar DW, Veitch NC, Williams RJP (1990) Eur J Biochem 192:715–721
14. Guiles RD, Sarma S, DiGate RJ, Banville D, Basus VJ, Kuntz ID, Waskell L (1996) Nat Struct Biol 3:333–339
15. Hom K, Ma QF, Wolfe G, Zhang H, Storch EM, Daggett V, Basus VJ, Waskell L (2000) Biochemistry 39:14025–14039
16. Barker PB, Bertini I, Del Conte R, Ferguson SJ, Hajieva P, Tomlinson EJ, Turano P, Viezzoli MS (2001) Eur J Biochem 268:4468–4476
17. Baistrocchi P, Banci L, Bertini I, Turano P, Bren KL, Gray HB (1996) Biochemistry 35:13788–13796
18. Banci L, Bertini I, Bren KL, Gray HB, Sompornpisut P, Turano P (1997) Biochemistry 36:8992–9001
19. Arnesano F, Banci L, Bertini I, Felli IC (1998) Biochemistry 37:173–184
20. Banci L, Bertini I, Rosato A, Scacchieri S (2000) Eur J Biochem 267:755–766
21. Palma PN, Krippahl L, Wampler JE, Moura JJG (2000) Proteins Struct Funct Genet 39:372–384
22. Morelli X, Dolla A, Czjzek M, Palma PN, Blasco F, Krippahl L, Moura JJG, Guerlesquin F (2000) Biochemistry 39:2530–2537
23. Morelli X, Czjzek M, Hatchikian C, Bornet O, Fontecilla-Camps JC, Palma PN, Moura JJG, Guerlesquin F (2001) J Biol Chem 275:23204–23210
24. Worrall JA, Liu A, Crowley PB, Nocek JM, Hoffman BM, Ubbink M (2002) Biochemistry 41:11721–11730
25. Crowley PB, Rabe KS, Worrall JA, Canters GW, Ubbink M (2002) ChemBioChem 3:526–533
26. Von Bodman SB, Schulder MA, Jollie DR, Sligar SG (1986) Proc Natl Acad Sci USA 83:9443–9447
27. Banci L, Bertini I, Felli IC, Hajieva P, Viezzoli MS (2001) J Biomol NMR 20:1–10
28. Arslan E, Schulz H, Zufferey R, Kuenzler P, Thoeny-Meyer L (1998) Biochem Biophys Res Commun 251:744–747
29. Pettigrew GW, Moore GR. (1987) Cytochromes c; biological aspects. Springer, Berlin Heidelberg New York
30. McLachlan SJ, La Mar GN, Burns PD, Smith KD, Langry KC (1986) Biochim Biophys Acta 874:274–284
31. Grzesiek S, Bax A (1992) J Am Chem Soc 114:6291–6293
32. Grzesiek S, Bax A (1992) J Magn Reson 99:201–207
33. Bodenhausen G, Ruben DJ (1980) Chem Phys Lett 69:185–188
34. Kay LE, Keifer P, Saarinen T (1992) J Am Chem Soc 114:10663–10665

35. Peng JW, Wagner G (1992) J Magn Reson 98:308–332
36. Kay LE, Torchia DA, Bax A (1989) Biochemistry 28:8972–8979
37. Grzesiek S, Bax A (1993) J Am Chem Soc 115:12593–12594
38. Brüschweiler R, Liao X, Wright PE (1995) Science 268:886–889
39. Lee LK, Rance M, Chazin WJ, Palmer AG III (1997) J Biomol NMR 9:287–298
40. Hwang TL, Van Zijl PCM, Mori S (1998) J Biomol NMR 11:221–226
41. Delaglio F, Grzesiek S, Vuister G, Zhu G, Pfeifer J, Bax A (1995) J Biomol NMR 6:277–293
42. Bartels C, Xia TH, Billeter M, Güntert P, Wüthrich K (1995) J Biomol NMR 5:1–10
43. Goddard TD, Kneller DG (2000) SPARKY 3. University of California, San Francisco
44. Grzesiek S, Bax A, Clore GM, Gronenborn AM, Hu J-S, Kaufman J, Palmer I, Stahl S, Wingfield P (1996) Nat Struct Biol 3:340–345
45. Garrett DS, Seok YJ, Peterkofsky A, Clore GM, Gronenborn AM (1997) Biochemistry 36:4393–4398
46. Pearlman DA, Case DA, Caldwell JW, Ross WS, Cheatham TE, Ferguson DM, Seibel GL, Singh UC, Weiner PK, Kollman PA. (1997) AMBER 5.0. University of California, San Francisco
47. Van Gunsteren WF, Berendsen HJC (1990) Angew Chem Int Ed Engl 298:992–1023
48. Banci L, Gori Savellini G, Turano P (1997) Eur J Biochem 249:716–723
49. Chothia C, Lesk AM (1985) J Mol Biol 182:151–158
50. Banci L, Bertini I, Rosato A, Varani G (1999) J Biol Inorg Chem 4:824–837
51. Tjandra N, Wingfield P, Stahl S, Bax A (1996) J Biomol NMR 8:273–284
52. Mauk MR, Reid LS, Mauk AG (1982) Biochemistry 21:1843–1846
53. Pollock WBR, Rosell FI, Twitchett MB, Dumont ME, Mauk AG (1998) Biochemistry 37:6124–6131
54. Morar AS, Kakouras DS, Young GB, Boyd J, Pielak G (1999) J Biol Inorg Chem 4:220–222
55. Schurr JM, Babcock HP, Fujimoto BS (1994) J Magn Reson Ser B 105:211–224
56. Zuiderweg ER (2002) Biochemistry 41:1–7
57. Whitford D (1992) Eur J Biochem 203:211–223
58. Fushman D, Xu R, Cowburn D (1999) Biochemistry 38:10225–10230
59. Pelletier H, Kraut J (1992) Science 258:1748–1755
60. Worrall JAR, Kolczak U, Canters GW, Ubbink M (2001) Biochemistry 40:7069–7076
61. Moore GR, Cox MC, Crowe D, Osborne MJ, Rosell FI, Bujons J, Barker PD, Mauk MR, Mauk AG (1998) Biochem J 332:439–449
62. Sun YL, Wang YH, Yan MM, Sun BY, Xie Y, Huang ZX, Jiang SK, Wu HM (1999) J Mol Biol 285:347–359
63. Qian C, Yao Y, Ye K, Wang J, Tang W, Wang Y, Wang W, Lu J, Xie Y, Huang Z (2001) Protein Sci 10:2451–2459
64. Wu Y, Wang Y, Qian C, Lu J, Li E, Wang W, Xie Y, Wang J, Zhu D, Huang Z, Tang W (2001) Eur J Biochem 268:1620–1630
65. Ng S, Smith MB, Smith HT, Millett F (1977) Biochemistry 16:4975–4978
66. Smith MB, Stonehuerner J, Ahmed AJ, Staudenmayer N, Millett F (1980) Biochim Biophys Acta 592:303–313
67. Rodriguez Maranon MJ, Qiu F, Stark RE, White SP, Zhang X, Foundling SI, Rodriguez V, Schilling CL, Bunce RA, Rivera M (1996) Biochemistry 35:16378–16390
68. van Amsterdam IM, Ubbink M, Einsle O, Messerschmidt A, Merli A, Cavazzini D, Rossi GL, Canters GW (2002) Nat Struct Biol 9:48–52